Electrode Array Position Guiding in Cochlea Based on Impedance Variation: Computational Study

Enver SALKIM

Electronic and Electrical Department, School of Technical Science, Biomedical Device Technology Group, Muş Alparslan University, Muş , Turkey

e-mail: e.salkim@alparslan.edu.tr

Abstract

The electro anatomy of the cochlea plays a crucial role in hearing, where damage to the cochlea may cause hearing loss. Cochlear neuromodulators provide hearing to severe or profound hearing-impaired individuals. The accurate insertion of electrodes into the cochlea is an important factor. If misplaced it may lead to further damage (insertion trauma). Visual inspection of the electrode insertion is limited and relies on the experience of the surgeon. Assisted real time guidance in positioning the electrode array in the cochlea during insertion is needed. Its position can be identified based on the variation in the impedances of electrodes which can be rapidly assessed and interpreted. Using an advanced computational model of the cochlea which accounted for different tissue layers in the cochlea, impedance variations and electrical potentials at different electrode distances from the cochlear wall were simulated, which suggest that the variations in impedance can be used to detect the proximity of the electrodes to the cochlea wall.

Keywords: Cochlear implant, computational models, electrical stimulation, electrode proximity, impedance measurement.

1. INTRODUCTION

The cochlea has a vital role in generating a sense of hearing. Sound vibrations are converted to nerve impulses by hair cells in the cochlea. These are transmitted to the brain through the auditory nerve to be processed. Damage to the hair cells in the cochlea leads to sensorineural hearing loss. A cochlear implant (CI) is a modern neural prosthesis designed to restore hearing loss by electrical stimulation of the auditory nerve fiber (as shown in Fig.1). Using an electrode array inserted in the scala tympani of the cochlea, the implant delivers modulated electric stimuli directly to the residual auditory nerve fibers, thus replacing the function of the damaged hair cells [1], [2].

The quality of restored hearing sensation is strongly related to the quality of surgery of CI implantation, particularly the optimum positioning of the electrode array inside the delicate cochlea without damage. It has been shown that the placement of the electrodes close to the auditory nerve fibers is of crucial importance for effective electrical stimulation, but if the electrode array touches the modiolar (cochlear wall) [3], [4] during the implantation procedure it may lead to damage and hearing loss. It has been shown that the location of the electrode array relative to the cochlear wall has a strong effect on the distribution of electrical signals and the excitation pattern of the auditory nerve [5], [6].

Currently, the visual inspection by the surgeon of the cochlear electrode array position is limited. Although post-operative computed tomography (CT) imaging is an option, it is not desirable due to the radiation risk [7]. The location of electrode array relative to the cochlear wall has a strong effect on the distribution of electrical signals and the excitation pattern on the auditory nerve [5], [6]. Positioning based on impedance measurement, which is non-invasive may be an option to monitor the proximity of the electrode array to the modiolar in real-time to prevent damage. For this it is necessary to relate impedance measurements to the distance of electrode array from the cochlea wall which is not feasible by experiment.

In this paper the proximity of the modiolar to the electrodes and the effect of tissue parameters [8], [9] by way of impedance measurements is investigated using a detailed computational modes. It is implemented using finite elements (FE) and models (FEM). It consists of a volume conductor model which represents different anatomical structures and the electrodes, by their conductivities and appropriate boundary conditions. To design more effective artificial CIs, micro CT (µCT) has been used to measure with high precision cochlea internal dimensions and assess the variability of different cochlea [10], [11]. For this study, a three-dimensional (3D) volume conductor model of the human cochlea was generated based on average statistical distributions of its layers which have been obtained from data sets. A 3D model of the electrode array was generated based on Advance Bionic electrodes (Hannover, Germany). The impact of the proximity variation of the electrodes in the scala tympani was evaluated to determine whether the position of the electrode array could be predicted from impedance measurements. It is noted that this work extension of the previous work [12].

In Section II materials and methods to generate the volume conductor and the subsequent investigations are described. The results and discussions are reported in Sections III and IV. Conclusions and future directions are discussed in Section V.
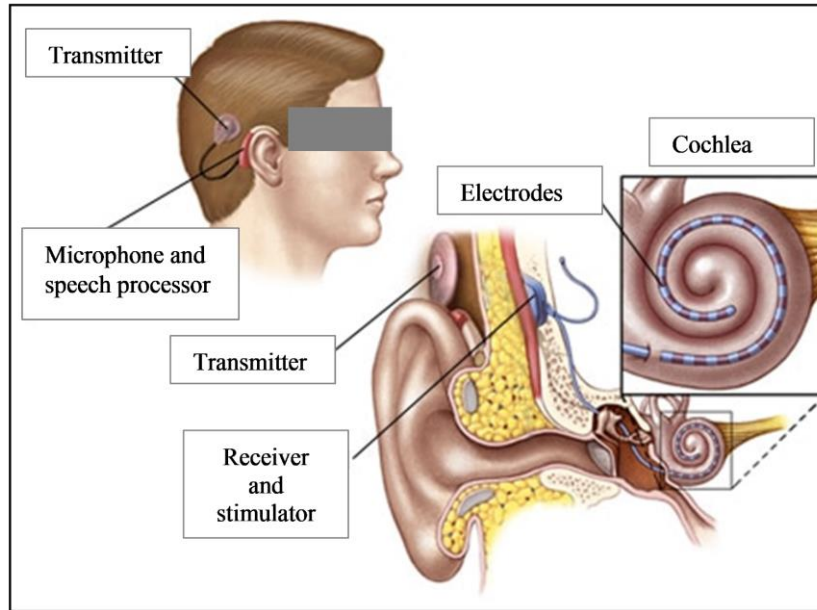
Fig.1. Components of the cochlear implant and full insertion of the electrode array in the cochlea are shown.
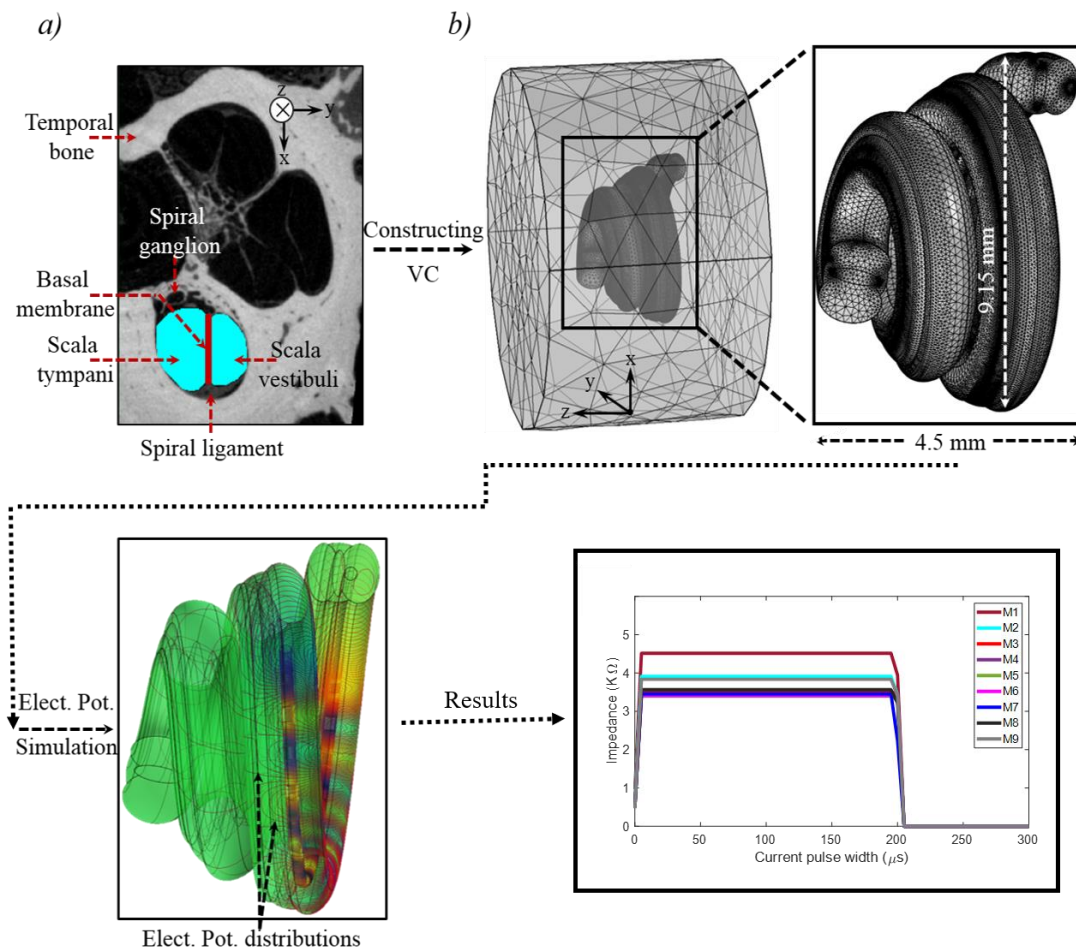

Fig.2. Cochlea and structures in vicinity modeling and electrical potential simulation. (a) The layers were modeled based on their average statistical values in COMSOL. (b) These models are then discretized and electrical potentials are solved using FEM. Since the thickness of the Stria vascularis is relatively small, it was incorporated in models as a boundary condition. The length of the first turn of the cochlea (9.15 mm) and total height (4.5 mm) are shown. The distributions of the electrical potentials within the volume conductor (VC) are shown.

2. MATERIALS AND METHODS

For all the subsequent simulations and operations, a computer with an Intel Core i7-6700 CPU@3.4 GHz with 64 GB RAM was used

2.1 Human Cochlea Modelling

The human cochlea volume conductor was developed based on the statistical distribution of the sample set of μCT data as shown in Fig.2a. As the electrode array is inserted into the scala tympani, it is crucial to include the tissue layers which are in vicinity in the volume conductor. Thus, scala tympani and vestibuli, basal membrane, spiral ligament and spiral ganglion were developed based their approximate statistical variations [11], [13]. The centre line of each layer was parameterised based on Archimedean spiral geometry using analytic equations and their derivatives. The spiral equations were converted from a polar to a Cartesian coordinate system to express each equation in a parametric form. This transformation allows modification of a set of desired parameters in the Cartesian coordinate system. The initial radius of the spiral (α_i), its final radius (α_f), and the desired number of turns (2.5 turns = 5π for an average cochlea model) were defined in COMSOL Multiphysics v5.5a (COMSOL, Ltd., Cambridge, U.K.). The spiral start and end angle were set based on the average statistical variation of the cochlea [11], [13]. In COMSOL, the work plane was defined by a parametric curve with associated Archimedean equations, as shown in Fig.3. Varying angles were entered into the parametric curve expression field to generate the Cartesian coordinates (*x, y, z*) using (1) to (4).

$$x = (\alpha + \beta * s) * cos(s) \qquad (1)$$

$$y = (\alpha + \beta * s) * sin(s) \qquad (2)$$

$$z = h_{max} * s/(\theta_f) \qquad (3)$$

$$\beta = \frac{\alpha_f - \alpha_i}{2\pi n} \qquad (4)$$

where, α is spiral radius, β the growth rate, *s* the varying parameter, h_{max} the length of the cochlea, θ_f the spiral final angle and *n* the turn numbers.

The 3D model of scala tympani and vestibuli were generated based on elliptic geometry with associated radii using a parametric sweep function by following a spiral curve in COMSOL Multiphysics. These functions were applied up to the average number of turns (2.5 turns = 5π) of the cochlea as shown in Fig.3. The remaining layers were constructed using similar functions and using Boolean operations to remove any intersections. Since it is not possible to observe the variation of the medium layer on the all data sets due to its thinness and the conductivity of this layer is similar to the vestibuli layer, it was modelled as a part of vestibuli layer. The thickness of the basilar membrane was doubled based on μCT data. The total length and total width (L×W=4.5×9.15 mm) of the cochlea were set to be slightly longer and wider to prevent self-intersection as indicated in Fig.2b. Bony structures were modelled in a smooth geometry to reduce the computation size as shown in Fig.2b. Since the fibrous tissue and bone
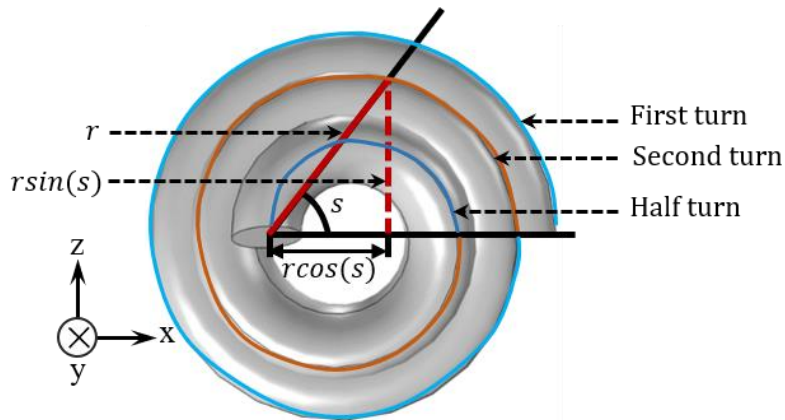

Fig.3. Generating of the 3D model of the scala tympani. The center line of the cochlea model was generated from an Archimedean spiral equation that can be described in both polar and Cartesian coordinates (*r*, $rsin(s), rcos(s)$). The associated equations are run for 5π, that is average turn of the human cochlea. The variation parameter shows with *s*.

layer have similar conductivity, the fibrous tissue was designed as a part of the bony structure. The stria vascularis layer is comparatively thin and was modelled as '*contact impedance*' during all simulations.

Table 1. Tissue Conductivities

Tissue layer	Conductivity (S/m)	Permittivity	Source
Scalas (Perilymph)	1.43	1	[18]
Basilar membrane	0.0125	1	[18]
Spiral ligament	1.67	1	[19]
Stria vascularis	0.005	1	[19]
Spiral ganglion	0.33	3556	[16]
Bone	0.0156	521.64	[18], [16]

2.2 Electrode Array Modelling

Electrodes were designed based on Advanced Bionic HiFocus Slim 1j charge-balanced electrode array that is equipped with platinum contacts to conduct stimulation currents to different parts of the cochlea as shown in Fig 4b. The electrode size (L×W=0.4×0.5 mm), the spacing between active contacts (~1.1 mm) and the total length of active contacts (~17 mm) were chosen from literature. Although the electrode tip and base diameter are different, the electrodes were designed using a base diameter (0.4 mm) in this study. The remainder of the array is composed of 16 contacts which are made of platinum and designed to face the cochlea wall, and soft silicone that supports the contacts (see Fig.4b). The electrode array was modelled inside the cochlea by interpolating the centre points of the scala tympani and using the sweep function in COMSOL. The centre point model was generated by calculating a variable cross-section of the scala tympani along with the spiral shape of the cochlea and stored as the *x, y* and *z* coordinates of the geometric centre of each cross-section. These were interpolated with a relatively high number in MATLAB v.R2019b (MathWorks, Inc., Natic M, USA) to obtain a smooth curve. Then, the data was imported to COMSOL to generate the 3D model of the electrode array using the sweep function. Since the thickness of the contacts is relatively thin, they were designed as a boundary surface. To parameterise the distance between the electrode array and cochlea wall, the electrode array was shifted in the *z*-direction with incremental steps (samples are shown in Fig.4a.) until the electrode array placed at the outer inside boundary of the scala tympani.
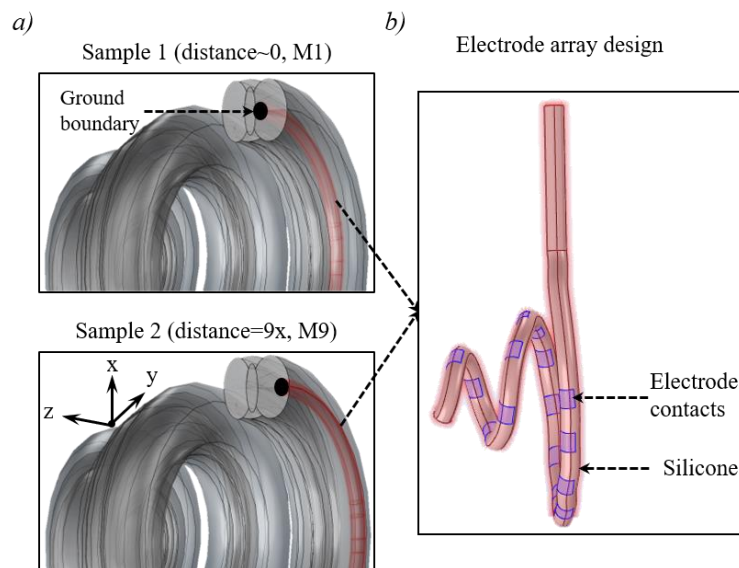

Fig.4. (a) Samples variations of the electrode array in the human average cochlea model. M shows model and numbers, x shows relative distance of the electrode array to the cochlear wall. The ground boundary is highlighted. Sample 1 shows the electrode array touched the cochlea wall and sample 2 represents the furthest model. (b) Electrode array design, the full electrode contacts (16 discrete contacts) are highlighted.

This resulted in nine different scenarios. The electrical potentials were simulated and the impedance variation along the cochlea wall was measured for each position. Note that an example electrode, Electrode 8, was used for all measurements.

2.3 Volume Conduction Simulation

FEM was used to calculate the electrical potentials within the volume conductor by discretising the domains using free tetrahedral elements. The regions of interest (mainly, electrode array, basilar membrane and scala tympani) were more finely meshed, while the rest of the region was relatively coarsely meshed to obtain more accurate potential distributions in a reasonable time. This resulted in 4 to 6 million tetrahedral elements and about 9 million degrees of freedom.

The time dependent electrical properties of the cochlea and the tissue layer in nearby have not been measured yet. Thus, only selected tissues with available comparable data (bone, nerve) were changed; the other tissues were left as they were in the resistive case. The conductivity and the permittivity of the bone and nerve were assigned based on available literature [14].

In this study, the models were simulated based on the time dependent electrical current approximation of Maxwell's equations. This is valid under condition assuming no free charge source (Q) and no external current density (J_e) in the volume conductor. By applying these conditions ($Q=0$, $J_e=0$) to equation (6) and (7), the Laplace equation (8) is obtained to calculate the electric potential distribution inside the conductive medium due to the injection of current via an electrode.

$$E = \nabla V \tag{5}$$

$$J = \sigma E + \frac{\partial D}{\partial t} + J_e \tag{6}$$

$$\nabla \cdot J = \nabla \cdot \left(\sigma \nabla V + \frac{\partial D}{\partial t} + J_e \right) = Q \tag{7}$$

$$\nabla \cdot \left(\sigma \nabla V + \frac{\partial D}{\partial t} \right) = 0 \tag{8}$$

where ∇ is the diverge operator, σ is the conductivity of layers, J is the current density, D indicates displacement, t is time and V and E are electrical potential and electrical field respectively.

In all models, 34 µA current pulse (200µs pulse duration) was applied through each electrode. This is the current recommended for conventional implants [12]. The current passes from cochlear electrode contacts through the surrounding medium and returns to the ground. The electrode-tissue interface contact impedance was assumed to be zero and appropriate continuity conditions were implemented at the boundary of the different domains to have a unique solution [8]. Although the available CIs neuromodulator was designed based on charge balanced rectangular current pulse, to reduce the computation cost the results were obtained based on the first pulse since there are identical results for both positive and negative pulses.

The outermost layer was as assumed to be air whose conductivity (σ=1e-10 S/m) was obtained from COMSOL library. The conductivities of remaining domains in the volume conductor are listed in Table 1 which were derived based on low frequencies. The conductivities of the tissue layers were assumed to be isotropic.

3. RESULTS

The potentials and impedance variation for the proximity of nine different electrode array settings to the cochlear wall based on the average cochlear model are shown in Fig.5. The variations in impedance and electrical potentials for all models are highlighted in different colours and labelled from model 1 (M1) to M9. The closest model (M1) variation is shown in a brown line, the variation for far position model (M9) from the cochlear wall indicated in a grey line and the variation for midscalar position model (M5) is shown green line for both electrical potential and impedance measurements.

It is clear that there is a direct relationship between electrode proximity to the cochlear wall and recorded impedance amplitudes. In general, the results showed that the impedance variation is increased as the electrode nears the cochlear wall. In particular, when the electrode array nearly touches the modiolar (distance to the cochlear wall ~ 0), the impedance variations significantly increased (highlighted in brown), compared to the remaining models. Even there is a distinguishable impedance difference between M2 and M3. The impedance variation for
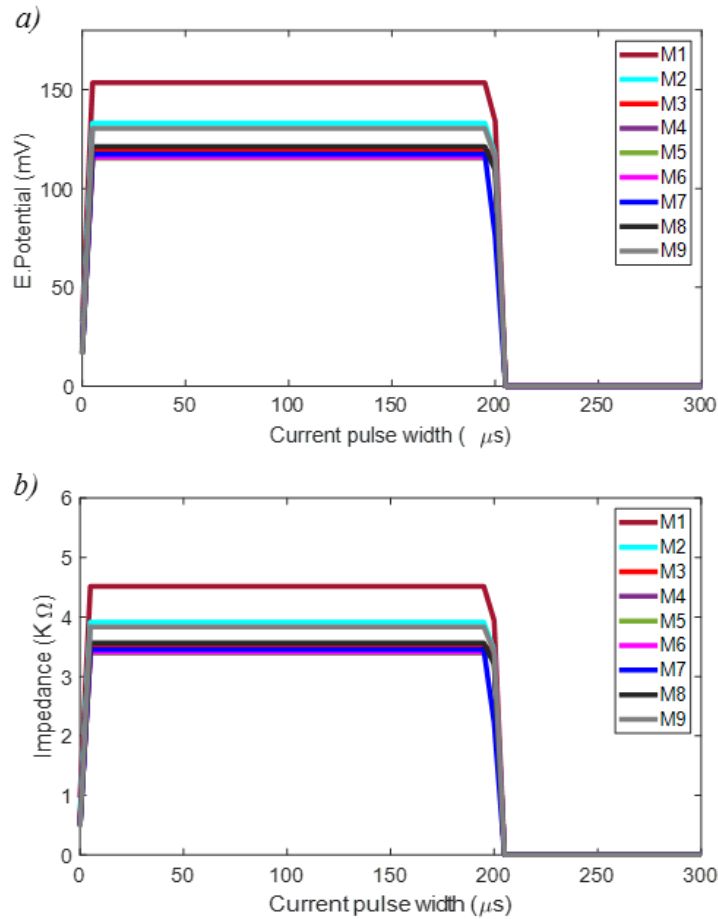
Fig.5. (a) Electrical potential variations on an electrode for proximities to the cochlear wall due to a current pulse of 34 µA. (b) Impedance variation versus different electrode array proximity to the cochlear wall. The variations were highlighted in different colors for different proximity to the cochlea wall. M represents the model numbers of the electrode array placed in the scala tympani with different proximity distance to the cochlear wall.

M3 to M8 (which are far from the edge of the scala tympani from both sides) shows similar and relatively lower variations.

Although the region of the interest is to evaluate the impedance variation based on the proximity of the cochlea wall, it was shown that if the electrode array is shifted far away in *z*- direction (distance = 9x, shown in Fig.4a) from the wall, and touched the other side of the scala tympani, the impedance variation also increased.

The current density along the cochlear wall was calculated based on CIs neuromodulator parameters using Eq. (6) and the results are shown in Fig.6. Fig.6a proves that the same electrode and the same current amount were used for all electrode models and the same computation criteria (e.g. meshing size) were used for all models as the results show the same variations for all models. The variation of the current density along the cochlea wall length is shown in Fig.6b. The result shows that the induced current density is within the safe limit for invasive stimulation for all electrode models [15]. As expected when the electrode is moved away from the cochlea wall, the current density at the wall is reduced.

4. DISCUSSION

The advanced computational modelling facilitates a depth and scale of the investigation that may not possible in experimental tests. Numerical methods have been used as a tool to study electrical stimulation within the volume conductors. The neuromodulator can be designed and developed using these sophisticated computational methods [5],[8],[9], [16].

In this study the volume conductor of the cochlea, the tissue layers in the vicinity and the implanted stimulation electrodes were constructed to analyse electrode impedance variations different electrode proximities to the cochlear wall. The results show the variation of impedance at different electrode positions in the scala tympani varied which is in agreement with the previous studies [7], [17]. However, the results showed a useful difference in impedance
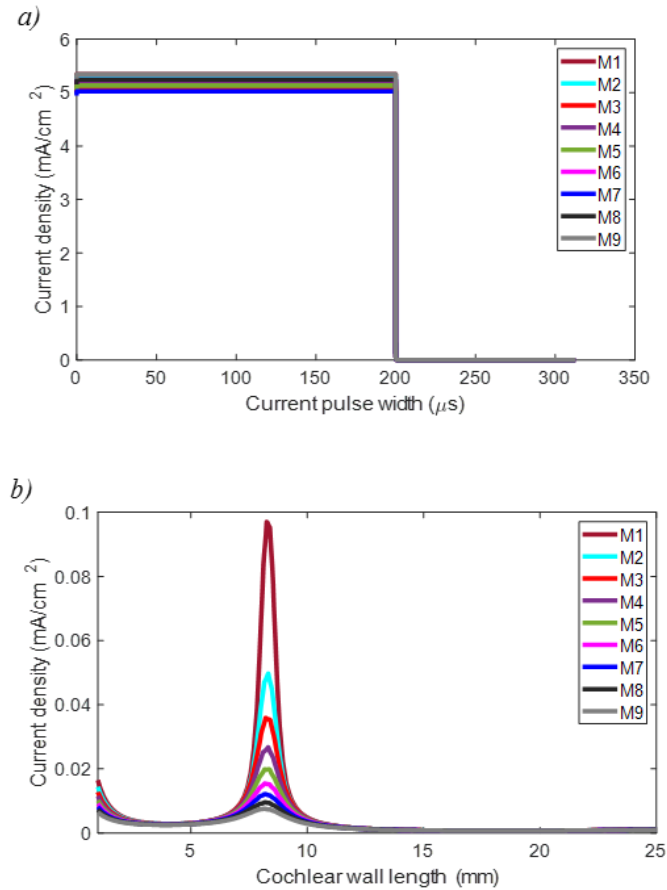
Fig.6. (a) Current density variation based on the stimulus current pulse for a specified electrode contact. (b) Current density variation along the cochlear wall for different electrode proximities to the cochlear wall. M represents the model numbers.

variation with proximity. Compared to the midscalar electrode model M5, M2 showed about 20% and M1 about 40% increase in impedance. This suggests that the variations in impedance can be used at a guide during electrode array insertion. However, the result has been obtained based on simplified cochlea modelling by considering only scala tympani in [7], and an average model of the cochlea was used to assess the impedance variations in this study. Also, these results were obtained based on post-processing. Using more detailed models generated based on μCT for different individuals that represent large group of people may result in more accurate impedance variation matrix to analyse if the electrode proximity to the cochlea wall can be detected based on impedance variations in a real time measurement.

It is crucial to consider charge safety limit during electrical stimulation. In general, charge-balanced stimulation is used to avoid any tissue or material damage. It was shown that the maximum current density is within the safe limit [15].

There is a compromise to be considered to either place the implant as close to the cochlea wall as possible to minimize current spread, or far from it to avoid cochlea wall insertion trauma [16]. These results provide quantitative evidence on the density when considering this.

5. CONCLUSION AND FUTURE WORK

A 3D finite element volume conductor of the cochlea was generated to guide the cochlear electrode array based on the impedance variation at different electrode proximities. The impedance variation was calculated using electrical stimulation through a cochlear implant electrode array. The results show that when an electrode is moved towards or away from the midscalar position, the impedance measurements are increased when an electrode was close to the cochlear wall, the impedance increased considerably. These characteristics suggest that the impedance measurement can actually guide the clinician to position the electrode in the cochlea to prevent to touch the sensitive structures (e.g. hair cells).

Although the results are promising, the anatomical layers in the cochlea and in its vicinity, which are used in the volume conductor model of the detailed human cochlea require further information from many different individuals to obtain more accurate results which will provide useful real time impedance measurements.

REFERENCES

1. A. Dhanasingh and C. Jolly, "An overview of cochlear implant electrode array designs," *Hear.Res.*, vol. 356, pp. 93–103, 2017.

2. K. Dang, "Electrical conduction models for cochlear implant stimulation," 2017.

3. L. K. Holden et al., "Factors affecting open-set word recognition in adults with cochlear implants," vol. 34, no. 3, pp. 342–360, 2014.

4. K. S. Min, S. B. Jun, Y. S. Lim, S. I. Park, and S. J. Kim, "Modiolus-hugging intracochlear electrode array with shape memory alloy," Comput. Math. Methods Med., vol. 2013, 2013.

5. T. H. and J. J. H. T. K. Malherbe, "Constructing a three- dimensional electrical model of a living cochlear implant user's cochlea," *Training*, vol. 4179, no. December 2015, p. 53, 2016.

6. J. H. M. Frijns, J. J. Briaire, and J. J. Grote, "The importance of human cochlear anatomy for the results of modiolus-hugging multichannel cochlear implants," *Otol. Neurotol.*, vol. 22, no. 3, pp. 340–349, 2001.

7. C. K. Giardina, E. S. Krause, K. Koka, and D. C. Fitzpatrick, "Impedance measures during invitro cochlear implantation predict array positioning," *IEEE Trans. Biomed. Eng.*, vol. 65, no. 2, pp. 327–335, 2018.

8. E. Salkim, A. Shiraz, and A. Demosthenous, "Impact of neuroanatomical variations and electrode orientation on stimulus current in a device for migraine: a computational study," *JNeural Eng.*, vol. 17, no. 1, p. 016006, 2019.

9. E. Salkim, A. Shiraz, and A. Demosthenous, "Influence of cellular structures of skin on fiber activation thresholds and computation cost In fl uence of cellular structures of skin on fi ber activation thresholds and computation cost," *Biomed. Phys. Eng. Express*, vol. 5, no. 1, p. 015015, 2018.

10. N. Gerber et al., "A multiscale imaging and modelling dataset of the human inner ear," Sci. data, vol. 4, p. 170132, 2017.

11. E. Avci, T. Nauwelaers, T. Lenarz, V. Hamacher, and A. Kral, "Variations in microanatomy of the human cochlea," *J. Comp. Neurol.*, vol. 522, no. 14, pp. 3245–3261, 2014.

12. E. Salkim, M. Zamani, and A. Demosthenous, "Detection of Electrode Proximity to the Cochlea Wall Based on Impedance Variation: a Preliminary Computational Study," *Int. J. Simul. Syst. Sci. Technol.*, vol. c, pp. 2–5, 2020.

13. E. Erixon, H. Högstorp, K. Wadin, and H. Rask-Andersen, "Variational anatomy of the human cochlea: Implications for cochlear implantation," *Otol. Neurotol.*, vol. 30, no. 1, pp. 14– 22, 2009.

14. P. Hasgall *et al.*, "IT'IS Database for thermal and electromagnetic parameters of biological tissues, Version 4.0," *IT'IS*, 01-Jan-2012. .

15. R. V Shannon, "A Model of Safe Levels for Electrical Stimulation," *IEEE T Bio-Med Eng*, vol. 39, no. 4, pp. 424–426, 1992.

16. T. Hanekom and J. J. Hanekom, "Three-dimensional models of cochlear implants: A review their development and how they could support management and maintenance of cochlear implant performance," *Network: Computation in Neural Systems*, vol. 27, no. 2–3. pp. 67–106, 2016.

17. J. Pile, A. D. Sweeney, S. Kumar, N. Simaan, and G. B. Wanna, "Detection of modiolar proximity through bipolar impedance measurements," *Laryngoscope*, vol. 127, no. 6, pp. 1413–1419, 2017.

18. C. C. Finley and M. W. White, "Models of Neural Responsiveness to Electrical Stimulation," Springer- Verlag, 1990, pp. 55–99.

19. J. H. M. Frijns, S. L. de Snoo, and R. Schoonhoven, "Potential distributions and neural excitation patterns in a rotationally symmetric model of the electrically stimulated cochlea," *Hear.Res.*, vol. 87, no. 1–2, pp. 170–186, 1995.